# Scalable Techniques for Autonomous Construction of a Paraboloidal Space Telescope in an Elliptic Orbit

Aaron John Sabu and Dwaipayan Mukherjee

***Abstract*— It is well acknowledged that human-made technology is not always at par with human curiosity, and an example is the inability to send large telescopes to outer space despite their higher resolution and less atmospheric interference. In this paper, we develop a framework for autonomous in-orbit construction using spacecraft formation such that a large telescope can be built in an elliptic orbit using multiple spacecraft. We split this problem into four steps for converging the position and attitude of each spacecraft at predefined values around a central spacecraft. Each spacecraft performs attitude synchronization with its neighbors to match its three degrees of freedom in orientation as a parabolic mirror. Simulations validate our proposed methods and the paper concludes with an open possibility of using other techniques to improve upon existing results.**

## I. INTRODUCTION

Since the first spacecraft (s/c) docking between Gemini 8 and an Agena Target Vehicle in 1966, in-space rendezvous and docking have been performed multiple times. This helped a few years later for the first men on the Moon to return from the Lunar Module to the Command Module and it helped make peace between two rivaling superpowers via the Apollo–Soyuz mission. Over time, it has been extended to the assembly of megastructures such as space stations.

Although the first space station, Salyut 1, was sent as a single piece to space, larger space stations such as Mir and the International Space Station (ISS) had modular designs and were assembled via docking of new modules with the space station using teleoperated robotic arms (Mir: Lyappa arm, ISS: Canadarm2/SSRMS) and/or extra-vehicular activity (EVA) [1]. The skill and experience of trained astronauts helped achieve quite complex assembly operations.

Treading along similar lines, we extend in-space assembly to large segmented space telescopes. The motivation for building larger telescopes arises from the decrease in exposure time to reach a given signal-to-noise ratio for a fixed resolution. Constructing the primary mirror out of segments, instead of a monolithic piece of glass, can drastically reduce the mirror mass and material costs [2]. This also makes transportation more feasible both on ground and to orbit.

The James Webb Space Telescope [3] intends to perform autonomous deployment in space using the technique of origami. The primary mirror segments are not separated. Instead, the horizontally outer segments are folded backwards and the sun shield is folded into the central section to reduce the size of the telescope for launch. However, folding is not a feasible option for a telescope that is much larger than the launch vehicle fairing. The volume taken by the folded telescope is almost equal to that of the unfolded telescope. Also, there is a huge uncertainty regarding the preservation of the exact shape that is expected from the mirror.

As a result, the most viable option is to adopt a design with separated segments. Although it is possible to assemble large telescopes manually via multiple EVAs, assembling a large telescope with multiple segments involves redundant activities that suit the application of autonomy. The use of robotic arms can be extended to fully autonomous assembly in which they carry segments to suitable locations and help them align with other segments. This has been proposed for the In-Space Astronomical Telescope (iSAT, [4], [5]), the Modern Universe Space Telescope (MUST, [6]) mission, and the In-Space Telescope Assembly Robotics (ISTAR, [7]). The Assembly of a Large Modular Optical Telescope (ALMOST, [8], [9]) also depends on external robotic agents for the placement of mirror segments at suitable locations. However, the use of a single robotic arm heavily constrains the speed of construction. Also, using multiple arms increases the problem complexity and poses threats of collisions.

Researchers have recently developed the concept of in-space construction of megastructures using s/c assembly by autonomous rendezvous and docking. Ref. [10] presents such a concept that includes the placement of s/c carrying mirror segments at suitable locations followed by tether-based docking. This technique is ideal for the purpose of in-space assembly since each s/c independently reaches its location without the need for robotic arms or other ‘movers’. However, the mentioned paper dealt with construction in a circular orbit and not an elliptical one, collision avoidance was not explicitly considered, and there was little discussion on s/c attitude dynamics.

Hence, in the light of these existing techniques, we propose a framework of algorithms for the autonomous construction of a telescope in an elliptic orbit. Sec. II provides prerequisites that are useful throughout the study. We consider a system with a central s/c that hosts the central telescope segment and other s/c that host an off-axis segment each (Sec. III-A). Some salient features of the framework are as follows:

- Each s/c establishes communication with neighboring s/c after ejection from the launch vehicle and converges to *unorganized pre-assembly* (Sec. III-B).
- These locations may be mismatched for some or all s/c.

The work was supported in part by an ISRO funded project bearing code RD/0120-ISROC00-007. Aaron John Sabu (aaronjohnsabu1999@gmail.com) is an undergraduate student and Dwaipayan Mukherjee (dm@ee.iitb.ac.in) is an Asst. Professor with the Dept. of Electrical Engineering, Indian Institute of Technology Bombay, Powai, Mumbai, Maharashtra, India

Such s/c are re-assigned to matching locations, leading to an *organized pre-assembly* (Sec. III-C).
- Each s/c synchronizes its attitude with neighboring s/c in the local reference frame. Subject to a switching communication topology, *attitude consensus* (Sec. III-D) is performed via local interactions with neighbors.
- Finally, the s/c form an *assembly*, building the space telescope by docking with neighbors using tethers [10].

Sec. IV presents simulations that verify the working of the framework of algorithms and Sec. V concludes the paper.

## II. PRELIMINARIES

### A. Translation in an Elliptic Orbit

When multiple s/c move in almost identical orbits and are very close to each other, we may define the non-inertial Local-Vertical-Local-Horizontal (LVLH) frame of reference whose origin is fixed at and moving with the center of mass (cm) of the central s/c. This is in contrast to the Earth-centered inertial (ECI) frame which is considered the inertial frame of reference since its orientation is fixed with respect to stars. The relative motion of other s/c in the LVLH frame are calculated using the Euler-Hill equations [11].
We consider the space telescope to be built in an elliptic orbit; hence motion in the LVLH frame is governed by the Tschauner-Hempel (TH) equations [12]. The state transition matrix $\mathbf{\Phi}(t)$ from the Yamanaka-Ankersen (YA) solution [13] for the homogeneous version of TH equations is given as:

$$\mathbf{\Phi}(t) = \begin{bmatrix} \mathbf{\Phi}_{rr}(t) & \mathbf{\Phi}_{r\dot{r}}(t) \\ \mathbf{\Phi}_{\dot{r}r}(t) & \mathbf{\Phi}_{\dot{r}\dot{r}}(t) \end{bmatrix} \tag{1}$$

$$\implies \begin{cases} \boldsymbol{r}_t = \mathbf{\Phi}_{rr}(t)\boldsymbol{r}_0 + \mathbf{\Phi}_{r\dot{r}}(t)\dot{\boldsymbol{r}}_0 \\ \dot{\boldsymbol{r}}_t = \mathbf{\Phi}_{\dot{r}r}(t)\boldsymbol{r}_0 + \mathbf{\Phi}_{\dot{r}\dot{r}}(t)\dot{\boldsymbol{r}}_0 \end{cases} \tag{2}$$

### B. Multipulse Glideslope Algorithm

The classical two-impulse rendezvous algorithm propels a chaser s/c directly towards some final position. Its start velocity is varied by applying a particular value of delta-v (change in velocity: a measure of the impulse per unit of s/c mass that is required for a maneuver) obtained from the TH equations.
Consider the start position at time $t = 0$ to be $\boldsymbol{r}_0$ and the start velocity before the application of velocity change to be $\dot{\boldsymbol{r}}_0^-$. The velocity $\dot{\boldsymbol{r}}_0^+$ and the delta-v at $\boldsymbol{r}_0$ to arrive at the final position $\boldsymbol{r}_1$ in time $T$ is obtained as ( [14]):

$$\dot{\boldsymbol{r}}_0^+ = \Phi_{r\dot{r}}^{-1}(T)\left(\boldsymbol{r}_1 - \Phi_{rr}(T)\boldsymbol{r}_0\right) \tag{3}$$

$$\Delta \boldsymbol{V}_0 = \dot{\boldsymbol{r}}_0^+ - \dot{\boldsymbol{r}}_0^- \tag{4}$$

The arrival velocity $\dot{\boldsymbol{r}}_1(T)$ at $\boldsymbol{r}_1(T)$ is countered by a delta-v:

$$\dot{\boldsymbol{r}}_1(T) = \Phi_{\dot{r}r}(T)\boldsymbol{r}_0 + \Phi_{\dot{r}\dot{r}}(T)\dot{\boldsymbol{r}}_0^+ \tag{5}$$

$$\Delta \boldsymbol{V}_1(T) = -\dot{\boldsymbol{r}}_1(T) \tag{6}$$

Under the two-impulse rendezvous algorithm, the chaser follows a curvilinear path in the LVLH frame of the central s/c (target). While this does not affect positional convergence, it may lead to issues in communication and sensing. This can be resolved using the multipulse glideslope transfer [14], which invokes guidance based on an inbound glideslope (a straight path from the start location of the chaser s/c to the final location). Continuous travel on the glideslope requires continuous thrust application, which may not be a practical option. Instead, it makes jumps (in the LVLH frame) from one point on the glideslope to the next.

### C. Zavlanos-Spesivtsev-Pappas (ZSP) Auction Algorithm

Given two sets, one containing start locations and the other with end locations, the linear assignment problem deals with the assignment of at most one start point to each endpoint and at most one endpoint to each start point, i.e. a one-to-one matching between the start points and the endpoints, such that the sum of lengths of all such combinations (or 'total length') in the assignment is minimized.
Ref. [15] solves this problem for multiple agents with limited communication capabilities, and distributed computation and memory resources. It proposes the ZSP distributed auction algorithm based on the basic auction algorithm ( [16]) while only local information is available to each agent. This algorithm converges to an assignment that maximizes the total reward within a linear approximation of the optimal one. The ZSP algorithm can be implemented over all agents at each intermediate point of the glideslope trajectory to compute the optimal allocation for their next targets.

### D. Attitude Synchronization in a Switching Topology

Attitude synchronization is the problem of bringing multiple s/c attitudes into an agreement, i.e., aiming to maintain the relative attitude between s/c in a predefined manner. While control algorithms for the problem are typically applicable for fixed network topologies, the communication topology in our problem changes due to specific operations, as will be evident later in Sec. III-C. However, [17] proves the validity of the consensus algorithm for switching topologies that satisfy uniform joint connectivity, thereby allowing s/c to lose contact with others intermittently. As a result, each s/c can perform attitude synchronization via consensus even before reaching the unorganized pre-assembly stage, and attitude synchronization is guaranteed thereafter.

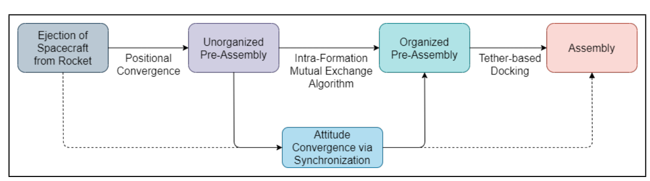


Fig. 1: Complete flowchart of various steps

### Problem Statement

We present a four-stage framework (Fig. 1) that can be implemented to construct a paraboloidal space telescope in an elliptic orbit around the earth. We consider a central s/c that hosts the on-axis segment of a large parabolic telescope and multiple s/c that individually host an off-axis segment.
- Each s/c forms a communication network with neighboring s/c after ejection into a mission-specific orbit and

subsequently converges using a hybrid algorithm (Sec. III-B.1) to one among a set of points representing the 'unorganized pre-assembly' configuration.

- These locations may be mismatched for some or all s/c due to variations in the off-axis parabolic mirror segments. These s/c are re-assigned to matching locations using a mutual exchange algorithm (Sec. III-C.1), leading to the 'organized pre-assembly' stage.
- Each s/c synchronizes its attitude with neighboring s/c in the local reference frame. Due to the switching nature of the communication topology, attitude consensus (Sec. III-D) is achieved via interactions with neighbors.
- Finally, the s/c form an 'assembly', building the space telescope using a technique similar to the tether-based docking ( [10]) to join with their neighbors.

The concept for intermediate pre-assembly followed by final assembly is inspired by [18] although the overall goal of that research is not aligned with our problem.

## III. MAIN RESULTS

### A. Parameterization of Off-Axis Paraboloidal (OAP) mirrors

Constructing a space telescope using s/c formation involves multiple s/c carrying off-axis segments of a paraboloidal mirror and assembling at predefined locations and attitudes around a central s/c that carries the central segment of the mirror. A hexagonal-segmented paraboloidal mirror is built up as 'rings' around the central segment (at ring 0). The $l$-th ring contains $6l$ segments and the total number of segments $N_{agents}$, excluding the central segment, is given in terms of the number of rings $N_{rings}$ [19]:

$$N_{agents} = 3N_{rings}\left(N_{rings}+1\right) \tag{7}$$

Consider a section of a paraboloid (Fig. 2) where the $z$ axis

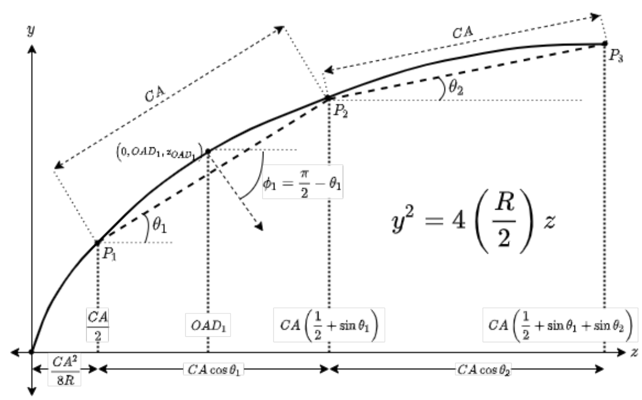


Fig. 2: Paraboloidal Mirror Cross-Section

and origin coincide with the reference optical axis (ROA) and the vertex of the paraboloid, respectively. The sink of the paraboloid of radius of curvature $R$ is given as ( [20]):

$$z(x,y) = \frac{x^2+y^2}{2R} \tag{8}$$

$$\text{or, } x^2+y^2 = 2Rz \tag{9}$$

The dotted straight line, the *aperture plane*, intersects with the $xy$ plane at $y = y_C$ at an angle $\theta$ to the $xz$-plane, and the section that it cuts out from the paraboloid represents the required OAP. We assume that all mirror segments have equal clear apertures (CA). Each s/c attaches to its OAP mirror segment at the aperture center $(0, \mathrm{OAD}_l, z_{\mathrm{OAD}_l})$, where the off-axis distance (OAD) is the normal distance from the ROA to this point. This point also lies on a tangent whose slope is equal to $\tan\theta_l$. From the standard relations of a parabola, this tangent can be written as $y = \frac{R}{\mathrm{OAD}_l}\left(z + z_{\mathrm{OAD}_l}\right)$ such that $\tan\theta_l = \frac{R}{\mathrm{OAD}_l}$. This gives us the $y$ and $z$ coordinates of the aperture center: $\mathrm{OAD}_l = \frac{R}{\tan\theta_l}$ and $z_{\mathrm{OAD}_l} = \frac{\mathrm{OAD}_l^2}{2R} = \frac{R}{2\tan^2\theta_l}$.

$P_l$, the lower boundary points of the segment of ring $l$ on the positive $yz$ plane can be solved for iteratively as:

$$P_l[z] = \frac{P_l[y]^2}{2R} \tag{10}$$

$$P_l \equiv \left(\mathrm{CA}\left(\frac{1}{2} + \sum_{i=1}^{l-1}\sin\theta_l\right),\ \mathrm{CA}\left(\frac{\mathrm{CA}}{8R} + \sum_{i=1}^{l-1}\cos\theta_l\right)\right) \tag{11}$$

While the $z$ coordinate of the remaining $N_l - 1$ segments on the ring is equal to that of segment 0, they form a symmetry around the central s/c such that their $x$ and $y$ coordinates are:

$$\left(P_{l,i}[x], P_{l,i}[y]\right) = P_{l,0}[y]\cdot\left(\sin\left(\frac{2\pi i}{N_l}\right),\ \cos\left(\frac{2\pi i}{N_l}\right)\right) \tag{12}$$

### B. Unorganized Pre-assembly

Following the ejection of s/c from the launch vehicle, they form a communication graph with neighbors based on a communication radius. To achieve the unorganized pre-assembly configuration, each s/c requires to translate from the point of ejection to one among a set of predefined locations in the LVLH frame of the central s/c. To prevent collisions, we may adopt a straight-trajectory collision avoidance technique.

*Lemma 1:* Two s/c considered in the LVLH frame cannot collide with each other if the two straight trajectories between their start and end points in an inertial frame do not intersect.

*Proof:* The collision of two s/c in the LVLH frame necessitates an intersection of the two curves connecting their start and end points in the LVLH frame at the same time $t = T$. Now, at $t = T$, the equivalent point $\boldsymbol{r}_{L,i}(T)$ of s/c $i$ in the LVLH frame for the point $\boldsymbol{r}_{I,i}(T)$ in the inertial frame is:

$$\boldsymbol{r}_{L,i}(T) = \boldsymbol{r}_{I,i}(T) - \int_{t_0}^{T} \boldsymbol{v}_{I,L}\,dt, \tag{13}$$

where $\boldsymbol{v}_{I,L}$ is the velocity of the LVLH frame with respect to the inertial frame. However, $\boldsymbol{v}_{I,L}$ is identical for both s/c since it depends solely on the motion of the central s/c and is independent of the individual s/c motions. Hence,

$$\boldsymbol{r}_{L,1}(T) = \boldsymbol{r}_{L,2}(T) \iff \boldsymbol{r}_{I,1}(T) = \boldsymbol{r}_{I,2}(T) \tag{14}$$

If the straight trajectories in the inertial frame do not intersect, two s/c can never occupy the same point in the inertial frame at the same time. However, this implies from Eqn.

(14) that the s/c do not occupy the same point at the same time in the LVLH frame. Hence, collisions are averted. □

From Lem. 1, considering non-intersecting straight trajectories for the motion of s/c will ensure collision avoidance between s/c. Hence, we may adopt the ZSP distributed auction algorithm (Sec. II-C).

*Theorem 1:* The ZSP distributed auction algorithm ensures the absence of intersecting lines by minimizing the total length of the configuration.

*Proof:* Suppose that a configuration contains an intersection at a point $P$ by the line segments $[A_s - A_e]$ and $[B_s - B_e]$ where $A_s, A_e$ are the start and end points for a segment and $B_s, B_e$ is the same for another. Now, we have

$$[A_s - A_e] \equiv [A_s - P] + [P - A_e] \tag{15}$$

$$\text{and } [B_s - B_e] \equiv [B_s - P] + [P - B_e]. \tag{16}$$

From the triangle inequality, we know that:

$$\text{len}([A_s - P]) + \text{len}([P - B_e]) > \text{len}([A_s - B_e]) \tag{17}$$

$$\text{and } \text{len}([B_s - P]) + \text{len}([P - A_e]) > \text{len}([B_s - A_e]) \tag{18}$$

Adding these inequalities, we see that $\text{len}[A_s - B_e] + \text{len}[B_s - A_e] < \text{len}[A_s - A_e] + \text{len}[B_s - B_e]$. Hence, the configuration with minimum total length cannot contain an intersection. Since the ZSP distributed auction algorithm returns the configuration with least total length for the assignment problem, it follows that it also ensures no intersecting lines. □

Although this algorithm inherently prevents collisions, it fails to be effective when the communication graph is not connected. Hence, we develop the distributed greedy algorithm where graph connectivity is not a requirement.

*1) Distributed Greedy Algorithm:* This algorithm, explained in Alg. 1, involves each s/c performing a myopic sequence of operations. If the trajectory of s/c $i$ intersects a neighbor's trajectory, their target locations are exchanged to resolve the intersection. Each s/c repeats this process until all intersections are resolved. Here, the boolean *intersecting* for s/c $i$ is 'True' if it has any intersection and *intNeighbors* is a list that enumerates the neighbors with intersecting lines.

Algorithm 1: Distributed Greedy Algorithm on agent $i$

**Input:** Init. Locations $R_0$, Init. Alloc. $R_T$, neighbors $N$
**Output:** Final Allocation $R_T$

**while** True **do**
  Compute *intNeighbors*, *intersecting* from $R_0$, $R_T$, $N$
  **if** intersecting **then**
    **for all** neighbor $j \in$ intNeighbors **do**
      Exchange $R_T[i]$ and $R_T[j]$
      Communicate change in $R_T$ with $N$
      Recompute intersecting, intNeighbors
      **if** not (intersecting[$i$]) **then**
        Exit the *for* loop
      **end if**
    **end for**
  **end if**
**end while**

*Lemma 2:* The distributed greedy algorithm for $n$ agents converges in finite time proportional to $n!$.

*Proof:* Solving the intersection between two straight trajectories by exchanging targets decreases the sum of lengths of the two lines (Thm. 1). This decreases the total length of all trajectories. The total length belongs to a discrete set of size $n!$. Hence, the algorithm will converge in finite time with worst time complexity of $n!$. □

*Theorem 2:* The distributed greedy algorithm prevents collisions between neighboring s/c and hence between all s/c if a s/c can potentially collide only with its neighbors.

*Proof:* From Thm. 1, we know that the configuration with least total length will not contain intersections. Now, the distributed greedy algorithm reduces the total length with each iteration. Since there is a finite number of permutations ($n!$) for straight trajectories, the final output of the algorithm will not contain intersections. Therefore, the distributed greedy algorithm prevents collisions between neighboring s/c (Lem. 1). It further prevents collision for all s/c if a s/c can potentially collide only with its neighbors. □

Sub-optimal solutions that do not contain intersections may exist and the greedy algorithm terminates once it reaches such a solution. Thus, the total length of straight trajectories may not be minimal. Hence, we propose a hybrid algorithm that runs the ZSP algorithm if the communication graph is connected and the distributed greedy algorithm otherwise.

### C. Organized Pre-assembly

Off-Axis Paraboloidal (OAP) mirrors are non-uniform; i.e., an OAP segment is identical in structure to another only if they belong to the same ring. Here, the ring number of an OAP segment is dictated by the quantity $l$ (Sec. III-A). As a result, a s/c carrying an OAP segment belonging to ring $l$ can only occupy a location among those in ring $l$.

This brings in the necessity for translating a mismatched s/c from its original location in the unorganized pre-assembly configuration to a location in the ring that it belongs to. An option that does not involve active s/c control is the use of space robot manipulators ( [21]) that may behave as standalone units or connected to the central s/c. However, such actuators tend to increase the cost and complexity of the system while also posing a threat to the fragile telescope segments. On the contrary, we propose that the s/c follow a simple exchange algorithm as depicted in Fig. 3.

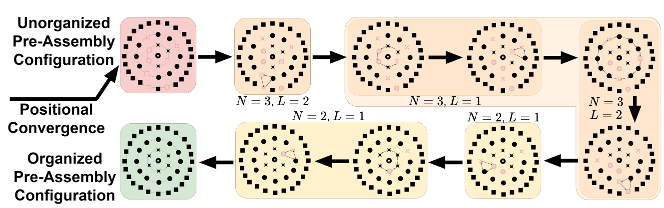


Fig. 3: Basic Flowchart of IFMEA

*1) Intra-Formation Mutual Exchange Algorithm:* IFMEA is a semi-decentralized algorithm that searches for and iteratively solves the closest mismatch that can be solved using the smallest number of exchanges and with the minimum

Algorithm 2: Intra-Formation Mutual Exchange Algorithm

**Input:** Init. Locations $R_0$, Unorganized Configuration $R_0$
**Output:** Organized Pre-assembly Configuration $R_T$

**for** $N \leftarrow \{maxN, \ldots, 1\}$ **do**
  **for** $L \leftarrow \{N-1, \ldots, 1\}$ **do**
    **while** $num(S_{N,L}) > 0$ **do**
      Pick a s/c $T \in S_{N,L}$
      **while** $l = ring(T) < N$ **do**
        Rotate $l$ bringing $T$ near $U \in S_{n,l+1}$, $n \neq l+1$
        Let $V$ be a neighbor of $U$ on $l+1$
        Exchange the s/c simultaneously as:
          S/c T $\rightarrow$ Loc. of V
          S/c V $\rightarrow$ Loc. of U
          S/c U $\rightarrow$ Loc. of T
      **end while**
    **end while**
  **end for**
**end for**

number of mismatches excluding the existing one. Let the ring number of the central s/c be 0. The algorithm is described in Alg. 2 where $maxN$ represents the maximum ring number; s/c belonging to the set $S_{N,L}$ ought to be in ring $N$ by virtue of their predefined geometry but are in ring $L$ by virtue of their current position; the function $num(S_{N,L})$ provides the number of s/c in the set $S_{N,L}$; and the function $ring(T)$ provides the present ring number of a s/c $T$.
If ring $L+1$ contains no mismatch, the s/c $T \in S_{N,L}$ is exchanged with an arbitrarily chosen s/c on ring $L+1$. This creates a new mismatch which will be resolved when $N = L+1$. Running the algorithm for a single mismatched s/c ensures the insertion of the ego s/c onto the outermost ring and the removal of another mismatched s/c from the ring. When run sequentially for all $S_{N,*}$, they are all brought to ring $N$. This process is repeated for lower levels until all the rings are filled with corresponding s/c. Hence, the sequential application of IFMEA for each s/c ensures its convergence.

### D. Attitude Consensus Algorithm

The communication topology of the pre-assembly stage is considered to be switching, undirected, and uniformly jointly connected. The central s/c maintains its own attitude at $(0,0,0)$ and the attitude of each other s/c needs to attain a predefined (fixed/varying) value. The roll of all s/c is set to zero since all segments of the telescope should be capable of docking along a line (edge of a hexagon). For a s/c at position $i$ of its present ring $m$ (with $N_m$ agents) and belonging to ring $l$, its pitch is the angle $\phi_l = \frac{\pi}{2} - \theta_l$ (Fig. 2) and its yaw is $\frac{2\pi i}{N_m}$ which varies with varying position.
While the pitch and roll of a s/c is consistent, its yaw depends on its position in the present ring. Hence, the steady-state value of yaw may vary over time during IFMEA. Each s/c $i$ follows attitude consensus according to Eqn. (19) within its neighborhood $\mathcal{N}_i$ where $p_i = q_i - q_{i,f}$ is its effective attitude, $q_i$ is its actual attitude, and $q_{i,f}$ is its required attitude (all angles are measured in its body frame $\mathscr{B}_i$).

$$p_{i,n+1} = \sum_{j \in \mathcal{N}_i} a_{ij} \left(p_{i,n} - p_{j,n}\right) \tag{19}$$

This can also be written in terms of actual s/c attitudes as:

$$q_{i,n+1} = \sum_{j \in \mathcal{N}_i} b_{ij} \left( \left(q_{i,n} - q_{i,f}\right) - \left(q_{j,n} - q_{j,f}\right) \right) + q_{i,f} \tag{20}$$

## IV. SIMULATIONS

We performed a simulation[1] demonstrating positional convergence to unorganized assembly followed by the intra-formation mutual exchange algorithm to organized assembly for a 3 m-radius segmented paraboloidal telescope with three rings that revolves around the Earth at a height of 400 km. Each segment has a clear aperture of 2 m.
A snapshot of convergence from a large radius of 5 km to a small radius of 10 m around the central s/c is shown in Fig. 5a, positional convergence is depicted in Fig. 5b, and the subsequent use of IFMEA is illustrated in Fig. 5c. All simulations are depicted in the LVLH frame of the central s/c. Fig. 5c does not show IFMEA rotations to reduce clutter although the simulations account for them. Although s/c that remain in the same positions are kept stationary in the plot, they will be in translation governed by the TH equations.
Fig. 6 represents the attitude synchronization of the s/c. We observe multiple transitions in yaw after reaching the first consensus due to IFMEA operations. This is not reflected in roll since its final value is zero for all s/c and not in pitch since its final value depends on the s/c's geometry.
We consider each s/c to be akin to a satellite (Fig. 4) that hosts a telescope segment on one side with tethers wound up at the opposite side. To prevent collisions, the pre-assembly locations are expanded versions of the actual positions computed from the OAP geometry. Following organized pre-assembly and attitude synchronization, each s/c ejects its tethers to dock with neighboring s/c following which they are drawn closer by mechanical and propulsive means.

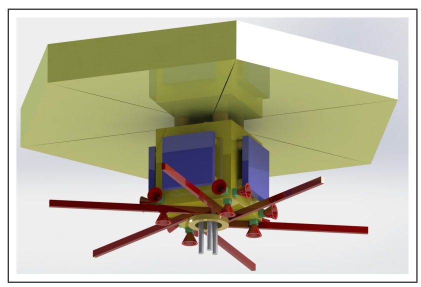

Fig. 4: The s/c in consideration (Bottom Dimetric View)

## V. CONCLUSION

We proposed a framework of algorithms for the autonomous assembly of spacecraft to construct a large-aperture telescope in space. We augmented the distributed greedy algorithm to the Zavlanos-Spesitsev-Pappas auction

[1]The code for the simulations is available at `https://github.com/aaronjohnsabu1999/tethered-self-assembly-AD2021`

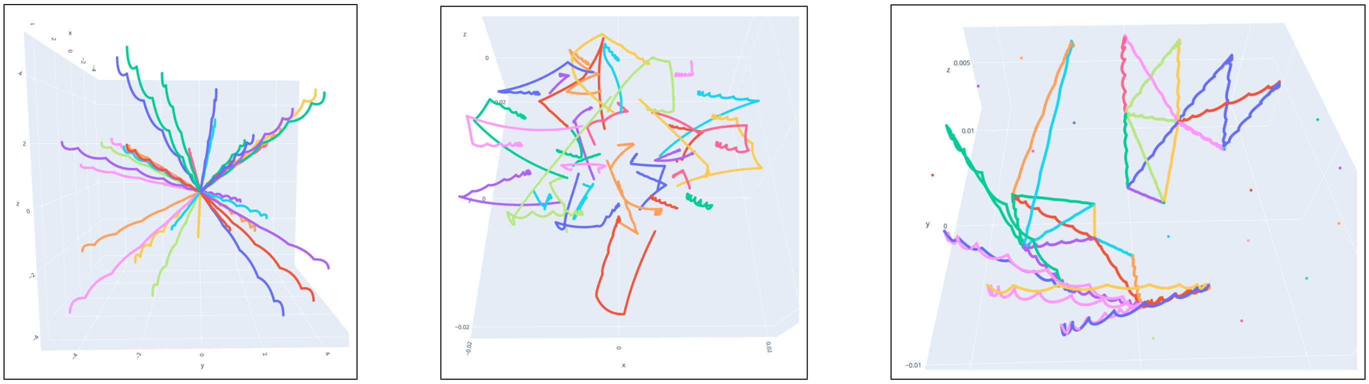

(a) Convergence to a small radius (b) Positional Convergence (c) IFMEA

Fig. 5: Spacecraft Formation using 36 (6+12+18) spacecraft: Steps 1A, 1B, and 2 (Position)

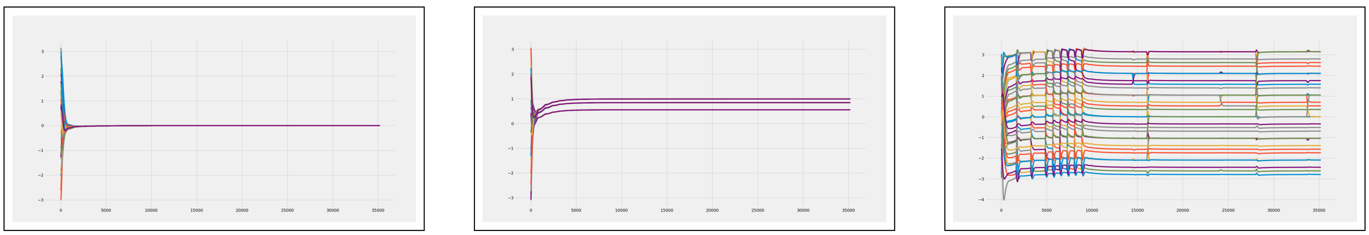

(a) Roll (b) Pitch (c) Yaw

Fig. 6: Spacecraft Formation using 36 (6+12+18) spacecraft: Step 3 (Attitude)

algorithm for positional convergence to unorganized pre-assembly. We further presented the intra-formation mutual exchange algorithm that performs layer rotations and triad exchanges to move misplaced spacecraft to their corresponding layer, thereby achieving organized pre-assembly which is followed by assembly via docking using tethers. We also achieved attitude synchronization of spacecraft via consensus with neighbors. Simulations in the LVLH frame of the central spacecraft verify the performance of the proposed algorithms. The future scope includes the adoption of decentralized reference frames and the generalization of IFMEA for telescopes with cyclic groups. Future studies may also incorporate non-homogeneous components, such as sunshields for mirror protection and trusses for structural integrity.

## References


[1] H. Ueno, T. Nishimaki, M. Oda, and N. Inaba, "Autonomous Cooperative Robots for Space Structure Assembly and Maintenance," *7th Int. Symp. Artif. Intell., Robot. and Automat. in Space*, 2003.

[2] T. Oswalt and I. S. McLean, *Planets, Stars and Stellar Systems - Volume 1: Telescopes and Instrum.* Springer Netherlands, 2013.

[3] M. Greenhouse, "The James Webb Space Telescope: Mission Overview and Status," in *2019 IEEE Aerosp. Conf.*, 2019.

[4] R. Mukherjee, N. Siegler, and H. Thronson, "The Future of Space Astronomy will be Built: Results from the In-Space Astronomical Telescope (iSAT) Assembly Design Study," 2019.

[5] G. Cataldo, M. Chodas, P. Dave, *et al.*, "Tradespace Investigation of a Telescope Architecture for Next-generation Space Astronomy and Exploration," 2014.

[6] D. Ebbets, J. DeCino, and J. Green, "Architecture Concept for a 10m UV-optical Space Telescope," in *Space Telescopes and Instrum.: Opt., Infrared, and Millimeter*, Int. Soc. Opt. and Photon. SPIE, 2006.

[7] K. Hogstrom, P. Backes, J. Burdick, *et al.*, "A Robotically-Assembled 100-Meter Space Telescope," *65th Int. Astronaut. Congress*, 2014.

[8] Z. Xue, J. Liu, C. Wu, and Y. Tong, "Review of In-Space Assembly Technologies," *Chinese J. Aeronaut.*, 2020.

[9] D. W. Miller, S. Mohan, and J. Budinoff, "Assembly of a Large Modular Optical Telescope (ALMOST)," in *Space Telescopes and Instrum.: Opt., Infrared, and Millimeter*, Int. Soc. Opt. and Photon. SPIE, 2008.

[10] R. C. Foust, Y. Nakka, A. Saxena, *et al.*, "Automated Rendezvous and Docking Using Tethered Formation Flight," *Int. Workshop Satell. Constellations Formation Flying*, 2017.

[11] M. J. Sidi, *Spacecraft Dynamics and Control: A Practical Engineering Approach*, ser. Cambridge Aerosp. Series, 1997.

[12] J. Tschauner and P. Hempel, "Optimale Beschleunigungsprogramme für das Rendezvous-Manöver," *Astronautica Acta*, vol. 10, 1964.

[13] K. Yamanaka and F. Ankersen, "New State Transition Matrix for Relative Motion on an Arbitrary Elliptical Orbit," *J. Guid., Control, and Dyn.*, vol. 25, no. 1, 2002.

[14] H. B. Hablani, M. L. Tapper, and D. J. Dana-Bashian, "Guidance and Relative Navigation for Autonomous Rendezvous in a Circular Orbit," *J. Guid., Control, and Dyn.*, vol. 25, no. 3, 2002.

[15] M. M. Zavlanos, L. Spesivtsev, and G. J. Pappas, "A Distributed Auction Algorithm for the Assignment Problem," in *2008 47th IEEE Conf. Decision and Control*, 2008.

[16] D. P. Bertsekas, "A New Algorithm for the Assignment Problem," *Mathematical Programming*, vol. 21, 1979.

[17] X. Liu, Y. Zou, Z. Meng, and Z. You, "Coordinated Attitude Synchronization and Tracking Control of Multiple Spacecraft Over a Communication Network With a Switching Topology," *IEEE Trans. Aerosp. and Electron. Syst.*, vol. 56, no. 2, 2020.

[18] T. Chen, H. Wen, H. Hu, and D. Jin, "On-Orbit Assembly of a Team of Flexible Spacecraft using Potential Field based Method," *Acta Astronautica*, vol. 133, 2017.

[19] P. Bely, *The Design and Construction of Large Optical Telescopes*. Springer-Verlag, 2003.

[20] J.-Y. Han, S. Lee, and D. W. Kim, "Parametric Geometry Analysis for Circular-aperture Off-axis Parabolic Mirror Segment," *J. Astronomical Telescopes, Instrum., and Syst.*, vol. 5, no. 2, 2019.

[21] Y. She, S. Li, Y. Liu, and M. Cao, "In-orbit Robotic Assembly Mission Design and Planning to construct a Large Space Telescope," *J. Astronomical Telescopes, Instrum., and Syst.*, vol. 6, no. 1, 2020.